Department of Veterans Affairs

Journal of Rehabilitation Research and Development Vol. 35 No. 2, June 1998
Pages 210–218

Kinematic characterization of wheelchair propulsion

Sean D. Shimada, PhD; Rick N. Robertson, PhD; Michael L. Bonninger, MD; Rory A. Cooper, PhD
Division of Physical Medicine and Rehabilitation, University of Pittsburgh Medical Center, Pittsburgh, PA 15261; Department of Rehabilitation Science and Technology, University of Pittsburgh, Pittsburgh, PA 15261; Human Engineering Research Laboratories, VA Pittsburgh Healthcare System, Pittsburgh, PA 15206

Abstract—Rehabilitation scientists and biomedical engineers have been investigating wheelchair propulsion biomechanics in order to prevent musculoskeletal injuries. Several studies have investigated wheelchair propulsion biomechanics; however, few have examined wheelchair propulsion stroke patterns. The purpose of this study was to characterize wheelchair propulsion stroke patterns by investigating joint accelerations, joint range of motions, wheelchair propulsion phases, and stroke efficiency.

Seven experienced wheelchair users (5 males, 2 females) were filmed using a three-camera motion analysis system. Each subject pushed a standard wheelchair fitted with a force-sensing pushrim (SMART^{Wheel}) at two speeds (1.3 and 2.2 m/s). The elbow angle was analyzed in the sagittal plane, while the shoulder joint was analyzed in the sagittal and frontal planes.

Three distinctly different stroke patterns: semi-circular (SC), single looping-over-propulsion (SLOP), and double looping-over-propulsion (DLOP), were identified from the kinematic analysis. Through our analysis of these patterns, we hypothesized that SC was more biomechanically efficient than the other stroke patterns. Future studies using a larger number of subjects and strokes may reveal more significant distinctions in efficiency measures between stroke patterns.

Key words: *biomechanics, kinematics, kinetics, stroke patterns, wheelchairs.*

This material is based upon work supported by the Department of Veterans Affairs Rehabilitation Research and Development Service, Washington, DC 20420 through the Edward Hines Jr. VA Hospital, the Paralyzed Veterans of America, and the VA Pittsburgh Healthcare System.

Address all correspondence and requests for reprints to: Sean D. Shimada, PhD, VA Medical Center (151-R1), Human Engineering Research Laboratories, Highland Drive, Pittsburgh, PA 15206; email: shimadas@hhsserver.hhs.csus.edu.

INTRODUCTION

Wheelchair propulsion by manual wheelchair users (MWUs) has been described as the bilateral, simultaneous, repetitive motion of the upper extremities (1). The repetitious nature of propelling a wheelchair has been associated with the high incidence of injury among MWUs (2,3). In addition to the repetitiveness, high forces and awkward postures have been associated with injuries such as carpal tunnel syndrome, tendinitis, and shoulder impingements (3–7). The high incidence of injury has led biomedical engineers and rehabilitation scientists toward the investigation of wheelchair propulsion biomechanics (8,9), a study that may ultimately provide insight into the mechanisms that cause musculoskeletal injury in MWUs.

A first step toward investigating injury mechanisms among MWUs is to define characteristic stroke patterns and explore their relationship to a number of biomechanical parameters, such as joint accelerations, joint range of motion (ROM), stroke efficiency, and wheelchair propulsion phases. Abrupt changes in joint angles can be detected through the analysis of joint accelerations, while extreme ROMs can be identified through large joint excursions. The analysis of propulsion phases may be used to identify inadequate time for force application, while stroke efficiency can be used to detect the extraneous forces that do not contribute to the forward motion of the wheelchair.

The purpose of this study was to characterize wheelchair propulsion stroke patterns through the investigation of joint accelerations, joint ROM, propulsion phases, and stroke efficiency.

Background

Sanderson and Sommer (10) were the first to investigate characteristic stroke patterns during wheelchair propulsion. Two distinct stroking styles were observed during an 80-min trial, defined as circular and pumping. The two subjects utilizing the circular had wrist trajectories that followed the path of the pushrim, while the subject who used the pumping technique had a short and abrupt stroking style that followed a small arc around the top of the pushrim. The abrupt braking and acceleration of the shoulder/arm complex observed during the pumping technique was hypothesized to cause slipping of the hand on the pushrim, contributing to the inefficiencies of the propulsion stroke. The MWUs who used circular stroking spent a larger percentage of their cycle time in propulsion, and stroked less frequently than the one with a pumping technique. Consequently, it was concluded that the circular style was more advantageous because of its prolonged propulsive phase, creating a greater impulse to the pushrim with less energy expenditure.

Chou et al. (11) investigated the kinematics of wheelchair propulsion by six subjects, three of whom were experienced MWUs and three ambulatory. The study revealed two stroking styles, circular and pumping: the circular stroking style was used by the efficient, experienced MWUs. The subjects with the pumping technique were found to be inefficient because of the abrupt change in motion during propulsion. The investigation did not use kinetic or physiologic data in order to quantify the efficiency of the stroke patterns. Only qualitative conclusions were made, supported by reference to Sanderson and Sommer's (10) findings.

Veeger et al. (12) investigated propulsion techniques at different speeds by five male wheelchair athletes, in order to investigate joint kinematics and gross mechanical efficiency (ratio of external power output and energetic cost). The kinematic analysis revealed a circular and pumping stroke pattern. No data were reported relating stroke patterns and joint kinematics, although the subjects with a circular stroke pattern did show a significantly higher gross mechanical efficiency than those with a pumping stroke pattern.

We feel that joint kinematics and pushrim kinetics are important biomechanical components that should be analyzed to further describe characteristic stroke patterns. Therefore, we will analyze both kinematic and kinetic measures, in order to characterize wheelchair propulsion stroke patterns.

METHODS

Subjects

A convenience sample of seven experienced MWUs (5 male, 2 female) with spinal cord injuries gave informed consent and volunteered for the study; all were athletes who had participated in the 1994 United States Olympic Committee's Wheelchair Sports USA Paralympic training camp. The athletes participated in a variety of sports including: table tennis, weight training, swimming, shooting, and wheelchair racing. The average age of the subjects was 31 years (range=22–42, SD=7.94).

Measurement System

Kinematic

A three-camera motion analysis system (Peak Performance Technologies, Inc., Englewood, CO), utilizing Panasonic Digital 5100 VHS video cameras, was used to collect kinematic data. The cameras were positioned at a 45° angle between the frontal and sagittal view, a frontal view with the camera 45° to the horizontal plane, and a sagittal view. The three optical axes of the cameras intersected at the center of the right wheelchair axle. Data were collected at 60 Hz with a shutter speed of 1/500 s. A pulse generated by the kinetic data collection system ensured that the video and kinetic data collection were synchronized.

Highly reflective spheres, used for digitizing purposes, identified five anatomical landmarks on each subject: the right greater trochanter, acromion process, lateral epicondyle, ulnar styloid process, and second metacarpophalangeal joint.

Kinetic

Kinetic data were obtained at 240 Hz using a 3-D force and torque sensing pushrim, the SMART^{Wheel}, to measure the forces and moments applied to the pushrim during propulsion. The characteristics and properties of the SMART^{Wheel} are throroughly described in the literature (9,13–15).

Experimental Protocol

Each subject pushed a standard wheelchair with a 0.41 m seat depth and width, 5° seat angle, and 95° backrest angle. The rear wheels were 61 cm in diameter, with a standard 53.3 cm pushrim, and adjusted to 0° camber. The wheelchair was fitted with a SMART^{Wheel} (9,13,14), then secured to a wheelchair dynamometer (16,17). The subjects were allowed to propel the

wheelchair on the dynamometer prior to the test trials in order to acclimate themselves to the experimental set-up. The subjects pushed the wheelchair for 3 min at 1.3 m/s and 2.2 m/s, resting approximately 1 min after each trial. Data were collected during the last 15 s of each trial.

Data Analysis

Kinematic

Each of the anatomical landmarks was digitized by the motion analysis system. The Peak5 Direct Linear Transformation (DLT) method was used to determine the relationship between the digitized coordinates from all camera views and the 3-D space coordinates. The DLT set-up file gave a digitized calibration frame measurement tolerance error of less than 0.2 percent. Since the error was within the 0.2 percent acceptable range, the DLT parameters were computed, completing the DLT. The 3-D data for each subject were conditioned with a 6 Hz, 8th-order Butterworth low-pass filter.

The elbow angle was analyzed in the sagittal plane (x-y plane), while the shoulder was analyzed in the sagittal and frontal plane (y-z plane). The sagittal and frontal planes were used to measure flexion/extension and abduction/adduction at the joint, respectively. The elbow at 180° is defined as full extension, with a decreasing angle as the elbow flexes. When the arm is in the reference anatomical position, the shoulder angle in the x-y plane is 0°. The shoulder x-y angle is positive when flexion occurs and negative when the joint moves into extension. The shoulder angle in the y-z plane is defined as 90° when the arm is abducted to the horizontal position. The shoulder y-z angle decreases as the arm adducts toward the mid-line. **Figures 1** and **2** illustrate the joint angle system used to define elbow and shoulder motion.

The angular displacement data calculated by the Peak5 motion analysis system were used to calculate elbow and shoulder joint ROMs and accelerations. Joint ROM for the elbow and shoulder were calculated as the difference between the maximum and minimum joint angle during one complete stroke. Joint accelerations were calculated as the second derivative of the joint displacement data acquired from the Peak5 system. The maximum angular acceleration values were obtained from one complete stroke. Mean values for elbow and shoulder joint ROM and angular accelerations were calculated for each subject during four complete strokes.

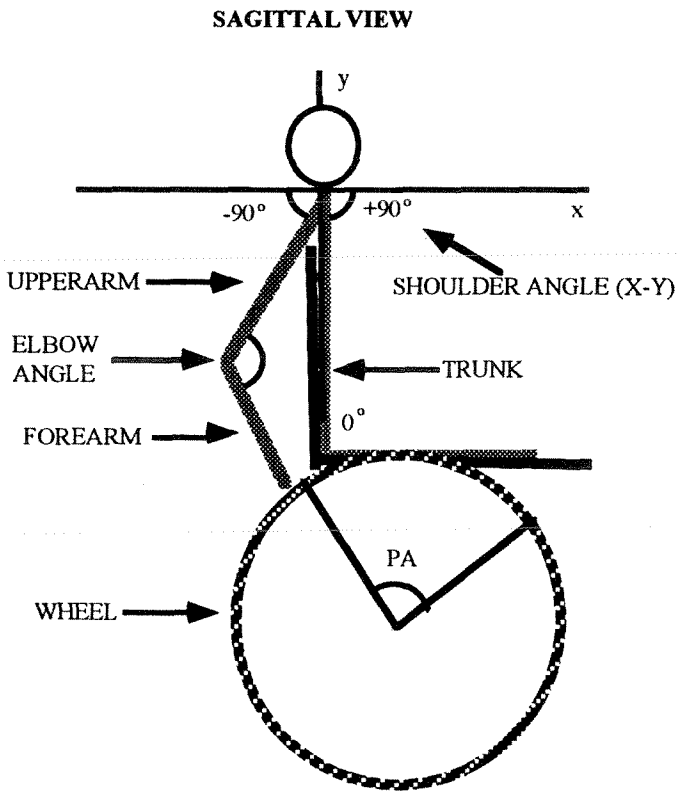

Figure 1.
Sagittal view of the shoulder and elbow angles used to describe elbow and shoulder joint motion during wheelchair propulsion.

Kinetic

The F_x, F_y, F_z, and M_z output from the SMART^{Wheel} were used for data analysis. F_x, F_y, F_z are the forces directed in the anterior/posterior, superior/inferior, and medial/lateral direction, respectively. M_z is the moment created about the wheelchair hub. The forces and moment are defined by the right-hand Cartesian coordinate system with respect to the laboratory coordinate system. The kinetic data from the SMART^{Wheel} were filtered with a 20 Hz, 12th-order Butterworth low-pass filter (18).

From the kinetic data, propulsion and recovery times were calculated as a percentage of cycle time (CT). The propulsion time (PT) was defined as the time when force was applied to the pushrim, while recovery time (RT) was defined as time when force measures returned to baseline values until the next application of force. The CT was calculated as the sum of PT and RT. Mean values for percent time spent in propulsion and recovery were calculated for each subject during four complete strokes.

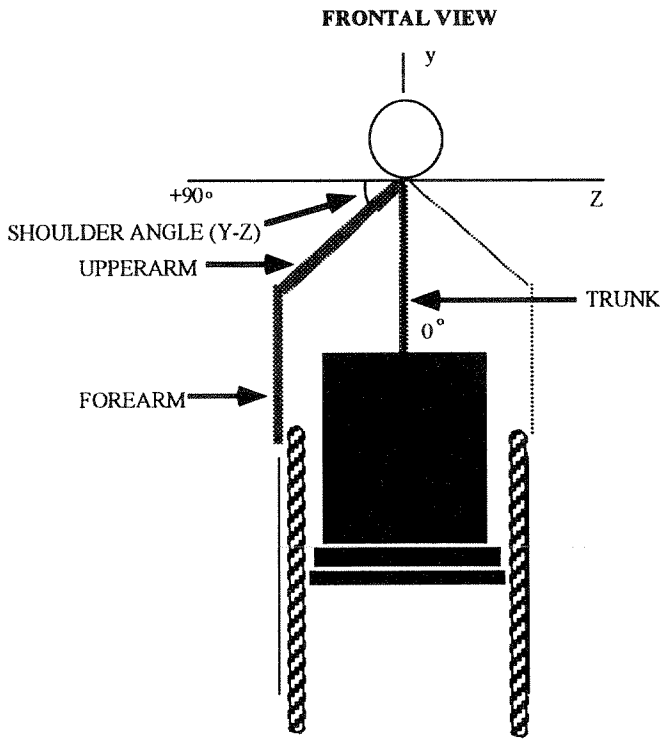

Figure 2.
Frontal view of the shoulder and elbow angles used to describe elbow and shoulder joint motion during wheelchair propulsion.

From the output data, the radial, tangential, and resultant forces applied to the pushrim were calculated. The resultant force (F) was defined as:

$$F = \sqrt{F_x^2 + F_y^2 + F_z^2}, \quad [1]$$

while, the tangential force (F_t) was defined as:

$$F_t = \frac{M_z}{r}, \quad [2]$$

where r is the radius of the pushrim.

From F_z, F_t, and F, F_r was calculated as:

$$F_r = \sqrt{F^2 - F_t^2 - F_z^2} \quad [3]$$

These values were defined in order to calculate stroke efficiency as a function of the radial, tangential, and resultant forces. The following equation was used to obtain a measure of stroke efficiency:

$$\frac{F_z^2}{F^2} + \frac{Fr^2}{F^2} + \frac{F_t^2}{F^2} = 1 \quad [4]$$

Since F_t is the only force that contributes to forward motion of the wheelchair, $\frac{F_t^2}{F^2}$ is a measure of stroke efficiency (15). The mean of $\frac{F_t^2}{F^2}$ during four consecutive propulsion strokes were calculated for each subject.

Statistical Analysis

A factorial ANOVA for joint accelerations, joint ROM, wheelchair propulsion phases, and stroke efficiency measures was used to detect differences between the three stroke patterns within speeds. The ANOVA for the three patterns represents both within and between subject variance. A Scheffe's post-hoc test using the same four measures was implemented with stroke patterns as the main effect and used to detect significant differences in measures between individual stroke patterns within speeds. The level of significance for the statistical tests was set at $p<0.05$.

RESULTS

Characteristic Stroke Patterns

From the kinematic data, three distinct stroke patterns were identified from the second metacarpophalangeal joint plots of the seven subjects: semicircular (SC), single looping over propulsion (SLOP), and double looping over propulsion (DLOP). The subjects using SC dropped their hands below the propulsion path during the recovery phase, while those using SLOP and DLOP lifted their hands *over* the propulsion path during that phase, hence the name. The motion of the hand during the recovery phase was the distinguishing feature between the SC and SLOP. The SLOP pattern was characterized by the subject not sharing a common coordinate during one complete stroke; those with a DLOP pattern had a characteristic cross-over point. **Figure 3** illustrates the three different stroke patterns identified through plotting the path of the second metacarpophalangeal joint during wheelchair propulsion.

Table 1 provides the distribution of stroke patterns for the seven subjects. Notice that all subjects except one maintained the same stroke pattern with increasing speed. Subject 7 changed from DLOP to SLOP when propulsion speed increased.

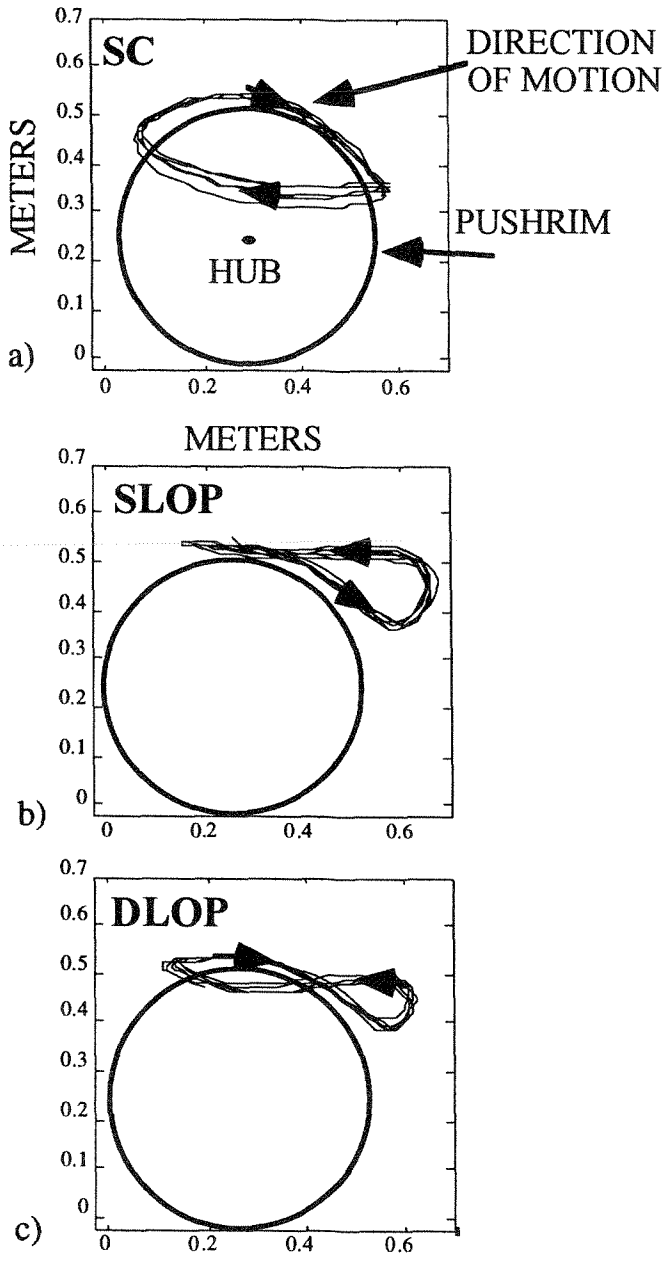

Figure 3.
Stroke patterns during the 1.3 m/s speed; a) semi-circular (SC); b) single looping over propulsion (SLOP); c) double looping over propulsion (DLOP).

Joint Accelerations

In order to quantify the changes in joint displacements within individual stroke patterns, mean maximum angular accelerations of the elbow and shoulder joints were calculated. **Table 2** reports this data for the three stroke patterns during both speeds.

Table 1.
Stroke patterns identified through the second metacarpophalangeal joint plots for the seven subjects during two speeds of wheelchair propulsion.

SUBJECT	STROKE PATTERN (1.3 m/s)	STROKE PATTERN (2.2 m/s)
1	SLOP	SLOP
2	DLOP	DLOP
3	DLOP	DLOP
4	SC	SC
5	SC	SC
6	DLOP	DLOP
7	DLOP	SLOP

SLOP=single looping-over-propulsion; DLOP=double looping-over-propulsion; SC=semi-circular.

The analysis of the elbow and shoulder joint only revealed significant ($p<0.05$) differences between stroke patterns during the 1.3 m/s speed. Specifically, subjects using SC had significantly smaller elbow flexion/extension joint accelerations and significantly smaller shoulder flexion/extension and larger abduction/adduction acceleration measures than those using DLOP, while those using DLOP had significantly larger shoulder flexion/extension accelerations than those using SLOP.

Joint Excursions

ROM measures for the elbow and shoulder joints were analyzed within each stroke pattern and are illustrated in **Figures 4** and **5.**

During both speeds of propulsion, significantly ($p<0.05$) larger elbow flexion/extension angles were found in subjects using SC than in those using the other stroke patterns. Those using DLOP had a significantly smaller shoulder flexion/extension angle than those using SLOP during the faster speed, and the DLOP stroke pattern also showed a significantly smaller shoulder abduction/adduction angle than did the other stroke patterns at the slower speed. During the fast speed, those using SC had shoulder abduction/adduction angles that were significantly larger than those of subjects using the other stroke patterns.

Wheelchair Propulsion Phases and Stroke Efficiency

The analyses of propulsion phases were reported as percentage of time spent in propulsion and recovery. **Table 3** provides the mean percent time spent in propulsion and recovery for the three patterns during both speeds. The analysis revealed that subjects using

Table 2.
Mean maximum joint accelerations for the three stroke patterns during the two speeds of propulsion.

STROKE PATTERN	SC		SLOP		DLOP	
SPEED	1.3 m/s (n=2)	2.2 m/s (n=2)	1.3 m/s (n=1)	2.2 m/s (n=2)	1.3 m/s (n=4)	2.2 m/s (n=3)
ELBOW*	5353.7	10384.4	5751.4	11298.1	6933.6	12723.5
(°/sec^2)	(1075.6)	(3010.2)	(597.0)	(2753.1)	(1089.2)	(2933.8)
SHOULDER X-Y*	2767.9	5877.2	2510.2	5614.1	3914.0	6267.7
(°/sec^2)	(367.6)	(1621.7)	(196.9)	(1118.7)	(1013.0)	(2101.6)
SHOULDER Y-Z*	3277.7	3921.9	4327.1	3817.1	2486.8	3732.1
(°/sec^2)	(1349.8)	(390.1)	(558.2)	(613.5)	(646.9)	(758.5)

*=significant differences found between stroke patterns at 1.3 m/s speed; numbers in parentheses represent standard deviation; SC=semi-circular; SLOP=single looping-over-propulsion; DLOP=double looping-over-propulsion.

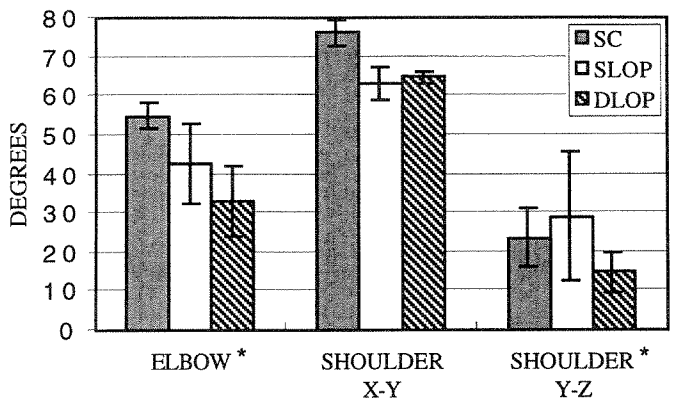

Figure 4.
Mean ROM measures for the elbow and shoulder joint for each of the stroke patterns during the 1.3 m/s speed. *=significant differences found between stroke patterns.

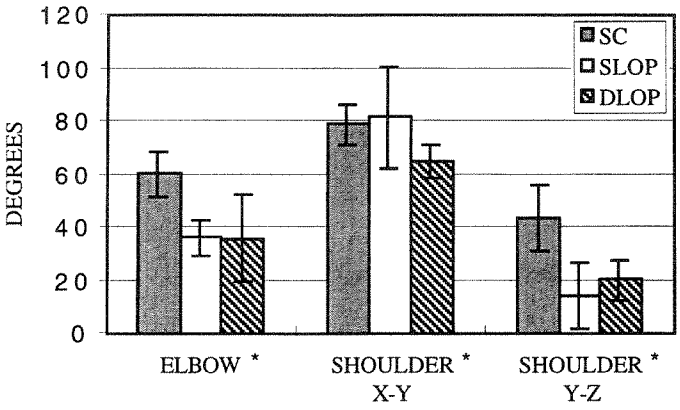

Figure 5.
Mean elbow and shoulder joint ROM measures for each stroke pattern during the 2.2 m/s speed. *=significant differences found between stroke patterns.

SC spent a significantly ($p<0.05$) longer percentage of their time in propulsion at both speeds than did users of the other two stroke patterns, and the SC stroke pattern had a significantly shorter time in recovery during the slower speed than did the SLOP pattern.

Stroke efficiency, defined by the mean of $\frac{F_t^2}{F^2}$, was calculated over four propulsion cycles for the three stroke patterns during the two speeds of propulsion. The results are listed in **Table 3.** No significant differences in stroke efficiency were found between the patterns during either speed.

DISCUSSION

The study of stroke patterns can lead us toward the identification of possible injury mechanisms in the manual wheelchair user. Associating characteristic stroke patterns with biomechanical measures could further strengthen the chances of identifying injury mechanisms. Because high accelerations (19–22), awkward postures (23–25), and extraneous forces (8,15) may contribute to injury, we investigated joint accelerations, joint ROMs, phase times, and stroke efficiency in order to quantify differences between stroke patterns.

Our study revealed three distinctly different stroke patterns, SC, SLOP, and DLOP, from the second metacarpophalangeal joint plots of seven subjects. Our SC pattern was similar to the circular stroke pattern reported in Chou et al. (11), Veeger et al. (12), and Sanderson and Sommer (10). The SLOP and DLOP patterns resembled the hand movement patterns illus-

Table 3.
Mean wheelchair propulsion phases and stroke efficiency measures for the three stroke patterns during two speeds of propulsion.

STROKE PATTERN	SC		SLOP		DLOP	
SPEED	1.3 m/s (n=2)	2.2 m/s (n=2)	1.3 m/s (n=1)	2.2 m/s (n=2)	1.3 m/s (n=4)	2.2 m/s (n=3)
PUSH TIME* #	42.12	32.60	32.64	24.25	32.63	29.79
(sec)	(3.99)	(1.75)	(4.52)	(5.41)	(5.22)	(6.49)
RECOVERY TIME* #	57.89	67.40	67.63	75.75	67.37	70.21
(sec)	(3.99)	(1.75)	(4.52)	(5.41)	(5.21)	(6.49)
$\frac{F_t^2}{F^2}$	0.714	0.705	0.645	0.598	0.644	0.626
	(0.035)	(0.082)	(0.046)	(0.106)	(0.087)	(0.071)

*=significant differences found between stroke patterns at 1.3 m/s speed; #=significant differences found between stroke patterns at 2.2 m/s speed; numbers in parentheses represent standard deviation; SC=semi-circular; SLOP=single looping-over-propulsion; DLOP=double looping-over-propulsion.

trated in Dallmeijer et al. (26), in which subjects with thoracic lesions had patterns similar to our subjects with the SLOP stroke pattern, while those with cervical lesions had a pattern comparable to the DLOP. Our three stroke patterns have been reported in previous studies (10–12,26). None of the our subjects exhibited the pumping stroke pattern reported by Sanderson and Sommer (10) and Chou et al. (11). The inexperienced and ambulatory subjects in their studies exhibited the pumping stroke pattern, while the experienced MWUs exhibited a circular stroke pattern (10,11). Therefore, it can be hypothesized that none of our subjects exhibited the pumping stroke pattern since we only studied experienced MWUs.

It has been reported that high joint accelerations contribute to injury (19–21). We quantified changes in joint angles through the analysis of joint accelerations, revealing that subjects with the SC pattern had smaller flexion/extension and shoulder abduction/adduction acceleration measures during the slower speed, when compared to the subjects with the DLOP and SLOP stroke patterns, respectively. The decreased acceleration seen in the individuals with a SC stroke pattern may lessen the risk of acceleration-related injuries.

The joint excursions were used in order to determine whether the joints were exposed to normal ROMs during propulsion. The results revealed that the subjects with the SC stroke pattern had significantly larger elbow and shoulder abduction/adduction ROMs when compared to the other stroke patterns. To determine whether the larger ROMs were injurious to these individuals, we examined their maximum and minimum elbow flexion/extension and shoulder abduction/adduction angles. The mean maximum elbow and shoulder abduction/adduction angles for these subjects were approximately 120 and 75°, respectively, during both speeds, and the minimum angles were approximately 80 and 35°, respectively. The maximum and minimum joint angles are well within normal ROMS (27); therefore, the larger ROMs found in subjects with a SC stroke pattern are not likely to contribute to injury.

Wheelchair propulsion phases were used to determine the length of time spent in propulsion, related to the time that force can be applied to the pushrim. Our analysis revealed that subjects with the SC pattern spent the greatest percentage of their CT in propulsion during both speeds, compared to those with other stroke patterns. Sanderson and Sommer (10) reported similar findings. When analyzing phases alone, it can be hypothesized that subjects using SC are more efficient, because a greater percentage of their CT is spent in propulsion, which, in turn, produces a larger impulse at the pushrim.

The final variable, stroke efficiency, was used to determine the proportion of the tangential force applied to the pushrim. In our application of wheelchair propulsion, all other forces do not contribute to forward motion. The analysis of stroke efficiency between all stroke patterns during both speeds did not reveal any statistical differences. Dallmeijer et al. (26) reported that subjects with lesion levels from C-4 to L-4 did not show any significant differences in fraction effective force (F_t/F) of the total force measures. It seems that the results from both investigations tend to support the notion that even though the magnitude of the resultant forces may vary from subject to subject, the percentage

used to maintain a given forward motion does not vary widely among experienced MWUs. Consequently, we could not make any conclusions regarding stroke patterns in relation to stroke efficiency. This may be due, in part, to the fact that stroke pattern characteristics are a function of the recovery phase, rather than the propulsion phase.

In order to quantify the effectiveness of the three stroke patterns using a multifactorial approach, **Table 4** provides information identifying the positive (+) and negative (−) attributes associated with each stroke pattern for both speeds of propulsion. The "±" symbol represents significant differences found between the given variable from the other stroke patterns, but no substantial conclusions were made regarding its being a positive or negative attribute. No symbol means that no significant differences were found, and, therefore, no conclusions apply.

Through our analysis of wheelchair propulsion stroke patterns, we hypothesized that the MWUs with the SC stroke pattern were more biomechanically efficient when propelling a wheelchair. These subjects had positive attributes, such as lower shoulder and elbow joint acceleration measures, along with a greater percentage of time spent in propulsion. These individuals may be less prone to injury because they apply less force to the pushrim over a greater amount of time. However, they did show a characteristic that we felt was not desirable, a larger elbow and shoulder ROM. We further examined their maximum and minimum joint angles and found that they were within normal ROMs (27). Therefore, we feel that the larger ROMs found in subjects exhibiting a SC stroke pattern does not predispose them to injury.

It can be seen that the differences between the stroke patterns primarily exist in the recovery phases. This is not surprising, since the hand is confined to the pushrim during propulsion. The recovery phase can exhibit many characteristics, since the hand can go through an infinite number of paths, given the large degree of freedom the shoulder/arm complex provides. Hence, the recovery phase of the wheelchair stroke cycle may be of future interest when investigating the efficiency of stroke patterns.

Table 4.
Positive and negative attributes associated with the three stroke patterns for both speeds of propulsion.

STROKE PATTERN	SC		SLOP		DLOP	
SPEED	1.3 m/s (n=2)	2.2 m/s (n=2)	1.3 m/s (n=1)	2.2 m/s (n=2)	1.3 m/s (n=4)	2.2 m/s (n=3)
ELBOW ACCEL	+				−	
SHOULDER X-Y ACCEL	+		+		−	
SHOULDER Y-Z ACCEL	−				+	
ELBOW ROM	±	±	±	±	±	±
SHOULDER X-Y ROM				±		±
SHOULDER Y-Z ROM		±	±	±	±	±
PUSH TIME	+	+	−	−	−	−
RECOVERY TIME	+		−			
$\frac{F_t^2}{F^2}$						

+=positive attribute associated with the given stroke pattern; −=negative attribute associated with the given stroke pattern; ±=significant differences found for the given parameter, but no conclusions can be made; no symbol=no positive or negative attributes apply; SC=semi-circular; SLOP=single looping-over-propulsion; DLOP=double looping-over-propulsion.

CONCLUSION

We hypothesized that the identification of the most efficient stroke pattern would lead us toward establishing a model for preventing injury of the MWU. From our multifactorial analysis, we concluded that the MWUs using the SC pattern were more biomechanically efficient than those with other stroke patterns. Because the seven subjects were separated into three categories, in one particular instance we were limited to one subject representing a stroke pattern. We were additionally limited to four complete strokes available for each subject. Consequently, we feel that the strength of our measures was reduced because of the small number of subjects and strokes representing each group. We anticipate future analyses of characteristic stroke patterns involving a larger group subjects with an increased number of strokes with the possibility of focus on the recovery phase.

REFERENCES

1. Davis R, Ferrara M. The competitive wheelchair stroke. Nat Strength Condition Assoc J 1988;10(3):4–10.
2. Gellman H, Chandler DR, Petrasek J, Sie I. Carpal tunnel syndrome in paraplegic patients. J Bone Joint Surg 1988;70A(4):517–9.
3. Apple DF, Cody R, Allen A. Overuse syndrome of the upper limb in people with spinal cord injury. In: Apple DF, editor. Physical fitness: a guide for individuals with spinal cord injury. J Rehabil Res Dev 1996;(Clin Suppl):97–108.
4. Armstrong TJ, Fine LJ, Goldstein SA, Lifshitz YR. Ergonomic considerations in hand and wrist tendinitis. J Hand Surg 1987;12A(5):830–7.
5. Silverstein BA, Fine LJ, Armstrong TJ. Occupational factors and carpal tunnel syndrome. Am J Ind Med 1987;11:343–58.
6. Silverstein BA, Fine LJ, Stetson D. Hand-wrist disorders among investment casting plant workers. J Hand Surg 1987;12A(5):838–44.
7. Silverstein BA, Fine LJ, Armstrong TJ. Hand wrist cumulative trauma disorders in industry. Br J Ind Med 1986;43:779–84.
8. Boninger ML, Cooper RA, Robertson RN, Rudy TE. Wrist biomechanics during two speeds of wheelchair propulsion: an analysis using a local coordinate system. Arch Phys Med Rehabil 1997;78:364–72.
9. Cooper RA, Robertson RN, VanSickle DP, Boninger ML. Methods for determining three-dimensional wheelchair pushrim forces and moments: a technical note. J Rehabil Res Dev 1997;34(2):162–70.
10. Sanderson DJ, Sommer HJ. Kinematic features of wheelchair propulsion. J Biomech 1985;18(6):423–9.
11. Chou YL, Su FC, An KN, Lu JW. Application of motion analysis system in analyzing wheelchair propulsion. Chin J Med Biol Eng 1991;11(4):173–7.
12. Veeger HEJ, van der Woude LHV, Rozendal RH. Wheelchair propulsion technique at different speeds. Scand J Rehabil Med 1989;21:197–203.
13. Asato KT, Cooper RA, Robertson RN, Ster JF. SMART^{Wheel}s: development and testing of a system for measuring manual wheelchair propulsion dynamics. IEEE Trans Biomed Eng 1993;40(12):1320–4.
14. VanSickle DP, Cooper RA, Robertson RN. SMART^{Wheel}: development of a digital force and moment sensing pushrim. Proceedings of RESNA International '95; 1995 Jun 9-14, Vancouver, BC. Washington, DC: RESNA Press; 1995. p. 352–4.
15. Robertson RN, Boninger ML, Cooper RA, Shimada SD. Pushrim forces and joint kinetics during wheelchair propulsion. Arch Phys Med Rehabil 1996;77:856–64.
16. Vosse A, Cooper R, Dhaliwal B. Computer control of a wheelchair dynamometer. Proceedings of the 13th Annual RESNA Conference; 1990 Jun 15-20, Washington, DC. Washington, DC: RESNA Press; 1990. p. 59–60.
17. Shimada SD, Cooper RA, Lawrence BM, Robertson RN. Computer controlled wheelchair dynamometer. Proceedings of the IEEE Engineering in Medicine and Biology 17th Annual Conference, Montreal; 1995. New York: IEEE Press; 1995. p. 427–8.
18. Cooper RA, DiGiovine CP, Boninger ML, Shimada SD. Frequency analysis of 3-dimensional pushrim forces and moments for manual wheelchair propulsion. Automedica. In press.
19. Glousman RE, Barron J, Jobe FW, Perry J. An electromyographic analysis of the elbow in normal and injured pitchers with medial collateral ligament insufficiency. Am J Sport Med 1992;20(3):311–7.
20. Fleisig GS, Andrews JR, Dillman CJ, Escamilla RF. Kinetics of baseball pitching with implications about injury mechanisms. Am J Sport Med 1995;23(2):233–9.
21. Marras WS. Toward an understanding of dynamic variables in ergonomics. Occup Med 1992;7(4):655–77.
22. Marras WS, Schoenmarklin RW. Wrist motion in industry. Ergonomics 1993;36(4):341–51.
23. Thurston AJ, Krause BL. The possible role of vascular congestion in carpal tunnel syndrome. J Hand Surg 1988;13B(4):397–9.
24. Feldman RG, Goldman R, Keyserling WM. Peripheral nerve entrapment syndromes and ergonomic factors. Am J Ind Med 1983;4:661–81.
25. Armstrong TJ, Foulke JA, Joseph BS, Goldstein SA. Analysis of cumulative trauma disorders in a poultry processing plant. Am Ind Hyg Assoc J 1982;45:103–16.
26. Dallmeijer AJ, Kappe YJ, Veeger DHEJ, Janssen TWJ, van der Woude LHV. Anaerobic power output and propulsion technique in spinal cord injured subjects during wheelchair ergometry. J Rehabil Res Dev 1994;31(2):120–8.
27. Magee, DJ. Shoulder. In: Orthopedic physical assessment. Philadelphia: WB Saunders Co.; 1992. p. 90–142.

Submitted for publication August 9, 1996. Accepted in revised form August 28, 1997.